FERMILAB-PUB-10-096-E

Search for WW and WZ resonances decaying to electron, missing E_T, and two jets in $p\bar{p}$ collisions at $\sqrt{s} = 1.96$ TeV.

T. Aaltonen,[24] J. Adelman,[14] B. Álvarez González[w],[12] S. Amerio[ee],[44] D. Amidei,[35] A. Anastassov,[39] A. Annovi,[20] J. Antos,[15] G. Apollinari,[18] J. Appel,[18] A. Apresyan,[49] T. Arisawa,[58] A. Artikov,[16] J. Asaadi,[54] W. Ashmanskas,[18] A. Attal,[4] A. Aurisano,[54] F. Azfar,[43] W. Badgett,[18] A. Barbaro-Galtieri,[29] V.E. Barnes,[49] B.A. Barnett,[26] P. Barria[gg],[47] P. Bartos,[15] G. Bauer,[33] P.-H. Beauchemin,[34] F. Bedeschi,[47] D. Beecher,[31] S. Behari,[26] G. Bellettini[ff],[47] J. Bellinger,[60] D. Benjamin,[17] A. Beretvas,[18] A. Bhatti,[51] M. Binkley*,[18] D. Bisello[ee],[44] I. Bizjak[kk],[31] R.E. Blair,[2] C. Blocker,[7] B. Blumenfeld,[26] A. Bocci,[17] A. Bodek,[50] V. Boisvert,[50] D. Bortoletto,[49] J. Boudreau,[48] A. Boveia,[11] B. Brau[a],[11] A. Bridgeman,[25] L. Brigliadori[dd],[6] C. Bromberg,[36] E. Brubaker,[14] J. Budagov,[16] H.S. Budd,[50] S. Budd,[25] K. Burkett,[18] G. Busetto[ee],[44] P. Bussey,[22] A. Buzatu,[34] K. L. Byrum,[2] S. Cabrera[y],[17] C. Calancha,[32] S. Camarda,[4] M. Campanelli,[31] M. Campbell,[35] F. Canelli[14],[18] A. Canepa,[46] B. Carls,[25] D. Carlsmith,[60] R. Carosi,[47] S. Carrillo[n],[19] S. Carron,[18] B. Casal,[12] M. Casarsa,[18] A. Castro[dd],[6] P. Catastini[gg],[47] D. Cauz,[55] V. Cavaliere[gg],[47] M. Cavalli-Sforza,[4] A. Cerri,[29] L. Cerrito[q],[31] S.H. Chang,[28] Y.C. Chen,[1] M. Chertok,[8] G. Chiarelli,[47] G. Chlachidze,[18] F. Chlebana,[18] K. Cho,[28] D. Chokheli,[16] J.P. Chou,[23] K. Chung[o],[18] W.H. Chung,[60] Y.S. Chung,[50] T. Chwalek,[27] C.I. Ciobanu,[45] M.A. Ciocci[gg],[47] A. Clark,[21] D. Clark,[7] G. Compostella,[44] M.E. Convery,[18] J. Conway,[8] M.Corbo,[45] M. Cordelli,[20] C.A. Cox,[8] D.J. Cox,[8] F. Crescioli[ff],[47] C. Cuenca Almenar,[61] J. Cuevas[w],[12] R. Culbertson,[18] J.C. Cully,[35] D. Dagenhart,[18] N. d'Ascenzo[v],[45] M. Datta,[18] T. Davies,[22] P. de Barbaro,[50] S. De Cecco,[52] A. Deisher,[29] G. De Lorenzo,[4] M. Dell'Orso[ff],[47] C. Deluca,[4] L. Demortier,[51] J. Deng[f],[17] M. Deninno,[6] M. d'Errico[ee],[44] A. Di Canto[ff],[47] B. Di Ruzza,[47] J.R. Dittmann,[5] M. D'Onofrio,[4] S. Donati[ff],[47] P. Dong,[18] T. Dorigo,[44] S. Dube,[53] K. Ebina,[58] A. Elagin,[54] R. Erbacher,[8] D. Errede,[25] S. Errede,[25] N. Ershaidat[cc],[45] R. Eusebi,[54] H.C. Fang,[29] S. Farrington,[43] W.T. Fedorko,[14] R.G. Feild,[61] M. Feindt,[27] J.P. Fernandez,[32] C. Ferrazza[hh],[47] R. Field,[19] G. Flanagan[s],[49] R. Forrest,[8] M.J. Frank,[5] M. Franklin,[23] J.C. Freeman,[18] I. Furic,[19] M. Gallinaro,[51] J. Galyardt,[13] F. Garberson,[11] J.E. Garcia,[21] A.F. Garfinkel,[49] P. Garosi[gg],[47] H. Gerberich,[25] D. Gerdes,[35] A. Gessler,[27] S. Giagu[ii],[52] V. Giakoumopoulou,[3] P. Giannetti,[47] K. Gibson,[48] J.L. Gimmell,[50] C.M. Ginsburg,[18] N. Giokaris,[3] M. Giordani[jj],[55] P. Giromini,[20] M. Giunta,[47] G. Giurgiu,[26] V. Glagolev,[16] D. Glenzinski,[18] M. Gold,[38] N. Goldschmidt,[19] A. Golossanov,[18] G. Gomez,[12] G. Gomez-Ceballos,[33] M. Goncharov,[33] O. González,[32] I. Gorelov,[38] A.T. Goshaw,[17] K. Goulianos,[51] A. Gresele[ee],[44] S. Grinstein,[4] C. Grosso-Pilcher,[14] R.C. Group,[18] U. Grundler,[25] J. Guimaraes da Costa,[23] Z. Gunay-Unalan,[36] C. Haber,[29] S.R. Hahn,[18] E. Halkiadakis,[53] B.-Y. Han,[50] J.Y. Han,[50] F. Happacher,[20] K. Hara,[56] D. Hare,[53] M. Hare,[57] R.F. Harr,[59] M. Hartz,[48] K. Hatakeyama,[5] C. Hays,[43] M. Heck,[27] J. Heinrich,[46] M. Herndon,[60] J. Heuser,[27] S. Hewamanage,[5] D. Hidas,[53] C.S. Hill[c],[11] D. Hirschbuehl,[27] A. Hocker,[18] S. Hou,[1] M. Houlden,[30] S.-C. Hsu,[29] R.E. Hughes,[40] M. Hurwitz,[14] U. Husemann,[61] M. Hussein,[36] J. Huston,[36] J. Incandela,[11] G. Introzzi,[47] M. Iori[ii],[52] A. Ivanov[p],[8] E. James,[18] D. Jang,[13] B. Jayatilaka,[17] E.J. Jeon,[28] M.K. Jha,[6] S. Jindariani,[18] W. Johnson,[8] M. Jones,[49] K.K. Joo,[28] S.Y. Jun,[13] J.E. Jung,[28] T.R. Junk,[18] T. Kamon,[54] D. Kar,[19] P.E. Karchin,[59] Y. Kato[m],[42] R. Kephart,[18] W. Ketchum,[14] J. Keung,[46] V. Khotilovich,[54] B. Kilminster,[18] D.H. Kim,[28] H.S. Kim,[28] H.W. Kim,[28] J.E. Kim,[28] M.J. Kim,[20] S.B. Kim,[28] S.H. Kim,[56] Y.K. Kim,[14] N. Kimura,[58] L. Kirsch,[7] S. Klimenko,[19] B.R. Ko,[17] K. Kondo,[58] D.J. Kong,[28] J. Konigsberg,[19] A. Korytov,[19] A.V. Kotwal,[17] M. Kreps,[27] J. Kroll,[46] D. Krop,[14] N. Krumnack,[5] M. Kruse,[17] V. Krutelyov,[11] T. Kuhr,[27] N.P. Kulkarni,[59] M. Kurata,[56] S. Kwang,[14] A.T. Laasanen,[49] S. Lami,[47] S. Lammel,[18] M. Lancaster,[31] R.L. Lander,[8] K. Lannon[u],[40] A. Lath,[53] G. Latino[gg],[47] I. Lazzizzera[ee],[44] T. LeCompte,[2] E. Lee,[54] H.S. Lee,[14] J.S. Lee,[28] S.W. Lee[x],[54] S. Leone,[47] J.D. Lewis,[18] C.-J. Lin,[29] J. Linacre,[43] M. Lindgren,[18] E. Lipeles,[46] A. Lister,[21] D.O. Litvintsev,[18] C. Liu,[48] T. Liu,[18] N.S. Lockyer,[46] A. Loginov,[61] L. Lovas,[15] D. Lucchesi[ee],[44] J. Lueck,[27] P. Lujan,[29] P. Lukens,[18] G. Lungu,[51] J. Lys,[29] R. Lysak,[15] D. MacQueen,[34] R. Madrak,[18] K. Maeshima,[18] K. Makhoul,[33] P. Maksimovic,[26] S. Malde,[43] S. Malik,[31] G. Manca[e],[30] A. Manousakis-Katsikakis,[3] F. Margaroli,[49] C. Marino,[27] C.P. Marino,[25] A. Martin,[61] V. Martin[k],[22] M. Martínez,[4] R. Martínez-Ballarín,[32] P. Mastrandrea,[52] M. Mathis,[26] M.E. Mattson,[59] P. Mazzanti,[6] K.S. McFarland,[50] P. McIntyre,[54] R. McNulty[j],[30] A. Mehta,[30] P. Mehtala,[24] A. Menzione,[47] C. Mesropian,[51] T. Miao,[18] D. Mietlicki,[35] N. Miladinovic,[7] R. Miller,[36] C. Mills,[23] M. Milnik,[27] A. Mitra,[1] G. Mitselmakher,[19] H. Miyake,[56] S. Moed,[23] N. Moggi,[6] M.N. Mondragon[n],[18] C.S. Moon,[28] R. Moore,[18] M.J. Morello,[47] J. Morlock,[27] P. Movilla Fernandez,[18]

J. Mülmenstädt,[29] A. Mukherjee,[18] Th. Muller,[27] P. Murat,[18] M. Mussini[dd],[6] J. Nachtman[o],[18] Y. Nagai,[56] J. Naganoma,[56] K. Nakamura,[56] I. Nakano,[41] A. Napier,[57] J. Nett,[60] C. Neu[aa],[46] M.S. Neubauer,[25] S. Neubauer,[27] J. Nielsen[g],[29] L. Nodulman,[2] M. Norman,[10] O. Norniella,[25] E. Nurse,[31] L. Oakes,[43] S.H. Oh,[17] Y.D. Oh,[28] I. Oksuzian,[19] T. Okusawa,[42] R. Orava,[24] K. Osterberg,[24] S. Pagan Griso[ee],[44] C. Pagliarone,[55] E. Palencia,[18] V. Papadimitriou,[18] A. Papaikonomou,[27] A.A. Paramanov,[2] B. Parks,[40] S. Pashapour,[34] J. Patrick,[18] G. Pauletta[jj],[55] M. Paulini,[13] C. Paus,[33] T. Peiffer,[27] D.E. Pellett,[8] A. Penzo,[55] T.J. Phillips,[17] G. Piacentino,[47] E. Pianori,[46] L. Pinera,[19] K. Pitts,[25] C. Plager,[9] L. Pondrom,[60] K. Potamianos,[49] O. Poukhov*,[16] F. Prokoshin[z],[16] A. Pronko,[18] F. Ptohos[i],[18] E. Pueschel,[13] G. Punzi[ff],[47] J. Pursley,[60] J. Rademacker[c],[43] A. Rahaman,[48] V. Ramakrishnan,[60] N. Ranjan,[49] I. Redondo,[32] P. Renton,[43] M. Renz,[27] M. Rescigno,[52] S. Richter,[27] F. Rimondi[dd],[6] L. Ristori,[47] A. Robson,[22] T. Rodrigo,[12] T. Rodriguez,[46] E. Rogers,[25] S. Rolli,[57] R. Roser,[18] M. Rossi,[55] R. Rossin,[11] P. Roy,[34] A. Ruiz,[12] J. Russ,[13] V. Rusu,[18] B. Rutherford,[18] H. Saarikko,[24] A. Safonov,[54] W.K. Sakumoto,[50] L. Santi[jj],[55] L. Sartori,[47] K. Sato,[56] V. Saveliev[v],[45] A. Savoy-Navarro,[45] P. Schlabach,[18] A. Schmidt,[27] E.E. Schmidt,[18] M.A. Schmidt,[14] M.P. Schmidt*,[61] M. Schmitt,[39] T. Schwarz,[8] L. Scodellaro,[12] A. Scribano[gg],[47] F. Scuri,[47] A. Sedov,[49] S. Seidel,[38] Y. Seiya,[42] A. Semenov,[16] L. Sexton-Kennedy,[18] F. Sforza[ff],[47] A. Sfyrla,[25] S.Z. Shalhout,[59] T. Shears,[30] P.F. Shepard,[48] M. Shimojima[t],[56] S. Shiraishi,[14] M. Shochet,[14] Y. Shon,[60] I. Shreyber,[37] A. Simonenko,[16] P. Sinervo,[34] A. Sisakyan,[16] A.J. Slaughter,[18] J. Slaunwhite,[40] K. Sliwa,[57] J.R. Smith,[8] F.D. Snider,[18] R. Snihur,[34] A. Soha,[18] S. Somalwar,[53] V. Sorin,[4] P. Squillacioti[gg],[47] M. Stanitzki,[61] R. St. Denis,[22] B. Stelzer,[34] O. Stelzer-Chilton,[34] D. Stentz,[39] J. Strologas,[38] G.L. Strycker,[35] J.S. Suh,[28] A. Sukhanov,[19] I. Suslov,[16] A. Taffard[f],[25] R. Takashima,[41] Y. Takeuchi,[56] R. Tanaka,[41] J. Tang,[14] M. Tecchio,[35] P.K. Teng,[1] J. Thom[h],[18] J. Thome,[13] G.A. Thompson,[25] E. Thomson,[46] P. Tipton,[61] P. Ttito-Guzmán,[32] S. Tkaczyk,[18] D. Toback,[54] S. Tokar,[15] K. Tollefson,[36] T. Tomura,[56] D. Tonelli,[18] S. Torre,[20] D. Torretta,[18] P. Totaro[jj],[55] M. Trovato[hh],[47] S.-Y. Tsai,[1] Y. Tu,[46] N. Turini[gg],[47] F. Ukegawa,[56] S. Uozumi,[28] N. van Remortel[b],[24] A. Varganov,[35] E. Vataga[hh],[47] F. Vázquez[n],[19] G. Velev,[18] C. Vellidis,[3] M. Vidal,[32] I. Vila,[12] R. Vilar,[12] M. Vogel,[38] I. Volobouev[x],[29] G. Volpi[ff],[47] P. Wagner,[46] R.G. Wagner,[2] R.L. Wagner,[18] W. Wagner[bb],[27] J. Wagner-Kuhr,[27] T. Wakisaka,[42] R. Wallny,[9] C. Wang,[17] S.M. Wang,[1] A. Warburton,[34] D. Waters,[31] M. Weinberger,[54] J. Weinelt,[27] W.C. Wester III,[18] B. Whitehouse,[57] D. Whiteson[f],[46] A.B. Wicklund,[2] E. Wicklund,[18] S. Wilbur,[14] G. Williams,[34] H.H. Williams,[46] P. Wilson,[18] B.L. Winer,[40] P. Wittich[h],[18] S. Wolbers,[18] C. Wolfe,[14] H. Wolfe,[40] T. Wright,[35] X. Wu,[21] F. Würthwein,[10] A. Yagil,[10] K. Yamamoto,[42] J. Yamaoka,[17] U.K. Yang[r],[14] Y.C. Yang,[28] W.M. Yao,[29] G.P. Yeh,[18] K. Yi[o],[18] J. Yoh,[18] K. Yorita,[58] T. Yoshida[l],[42] G.B. Yu,[17] I. Yu,[28] S.S. Yu,[18] J.C. Yun,[18] A. Zanetti,[55] Y. Zeng,[17] X. Zhang,[25] Y. Zheng[d],[9] and S. Zucchelli[dd6]

(CDF Collaboration†)

[1]*Institute of Physics, Academia Sinica, Taipei, Taiwan 11529, Republic of China*
[2]*Argonne National Laboratory, Argonne, Illinois 60439, USA*
[3]*University of Athens, 157 71 Athens, Greece*
[4]*Institut de Fisica d'Altes Energies, Universitat Autonoma de Barcelona, E-08193, Bellaterra (Barcelona), Spain*
[5]*Baylor University, Waco, Texas 76798, USA*
[6]*Istituto Nazionale di Fisica Nucleare Bologna,* [dd]*University of Bologna, I-40127 Bologna, Italy*
[7]*Brandeis University, Waltham, Massachusetts 02254, USA*
[8]*University of California, Davis, Davis, California 95616, USA*
[9]*University of California, Los Angeles, Los Angeles, California 90024, USA*
[10]*University of California, San Diego, La Jolla, California 92093, USA*
[11]*University of California, Santa Barbara, Santa Barbara, California 93106, USA*
[12]*Instituto de Fisica de Cantabria, CSIC-University of Cantabria, 39005 Santander, Spain*
[13]*Carnegie Mellon University, Pittsburgh, Pennsylvania 15213, USA*
[14]*Enrico Fermi Institute, University of Chicago, Chicago, Illinois 60637, USA*
[15]*Comenius University, 842 48 Bratislava, Slovakia; Institute of Experimental Physics, 040 01 Kosice, Slovakia*
[16]*Joint Institute for Nuclear Research, RU-141980 Dubna, Russia*
[17]*Duke University, Durham, North Carolina 27708, USA*
[18]*Fermi National Accelerator Laboratory, Batavia, Illinois 60510, USA*
[19]*University of Florida, Gainesville, Florida 32611, USA*
[20]*Laboratori Nazionali di Frascati, Istituto Nazionale di Fisica Nucleare, I-00044 Frascati, Italy*
[21]*University of Geneva, CH-1211 Geneva 4, Switzerland*
[22]*Glasgow University, Glasgow G12 8QQ, United Kingdom*
[23]*Harvard University, Cambridge, Massachusetts 02138, USA*

[24] Division of High Energy Physics, Department of Physics,
University of Helsinki and Helsinki Institute of Physics, FIN-00014, Helsinki, Finland
[25] University of Illinois, Urbana, Illinois 61801, USA
[26] The Johns Hopkins University, Baltimore, Maryland 21218, USA
[27] Institut für Experimentelle Kernphysik, Karlsruhe Institute of Technology, D-76131 Karlsruhe, Germany
[28] Center for High Energy Physics: Kyungpook National University,
Daegu 702-701, Korea; Seoul National University, Seoul 151-742,
Korea; Sungkyunkwan University, Suwon 440-746,
Korea; Korea Institute of Science and Technology Information,
Daejeon 305-806, Korea; Chonnam National University, Gwangju 500-757,
Korea; Chonbuk National University, Jeonju 561-756, Korea
[29] Ernest Orlando Lawrence Berkeley National Laboratory, Berkeley, California 94720, USA
[30] University of Liverpool, Liverpool L69 7ZE, United Kingdom
[31] University College London, London WC1E 6BT, United Kingdom
[32] Centro de Investigaciones Energeticas Medioambientales y Tecnologicas, E-28040 Madrid, Spain
[33] Massachusetts Institute of Technology, Cambridge, Massachusetts 02139, USA
[34] Institute of Particle Physics: McGill University, Montréal, Québec,
Canada H3A 2T8; Simon Fraser University, Burnaby, British Columbia,
Canada V5A 1S6; University of Toronto, Toronto, Ontario,
Canada M5S 1A7; and TRIUMF, Vancouver, British Columbia, Canada V6T 2A3
[35] University of Michigan, Ann Arbor, Michigan 48109, USA
[36] Michigan State University, East Lansing, Michigan 48824, USA
[37] Institution for Theoretical and Experimental Physics, ITEP, Moscow 117259, Russia
[38] University of New Mexico, Albuquerque, New Mexico 87131, USA
[39] Northwestern University, Evanston, Illinois 60208, USA
[40] The Ohio State University, Columbus, Ohio 43210, USA
[41] Okayama University, Okayama 700-8530, Japan
[42] Osaka City University, Osaka 588, Japan
[43] University of Oxford, Oxford OX1 3RH, United Kingdom
[44] Istituto Nazionale di Fisica Nucleare, Sezione di Padova-Trento, [ee] University of Padova, I-35131 Padova, Italy
[45] LPNHE, Universite Pierre et Marie Curie/IN2P3-CNRS, UMR7585, Paris, F-75252 France
[46] University of Pennsylvania, Philadelphia, Pennsylvania 19104, USA
[47] Istituto Nazionale di Fisica Nucleare Pisa, [ff] University of Pisa,
[gg] University of Siena and [hh] Scuola Normale Superiore, I-56127 Pisa, Italy
[48] University of Pittsburgh, Pittsburgh, Pennsylvania 15260, USA
[49] Purdue University, West Lafayette, Indiana 47907, USA
[50] University of Rochester, Rochester, New York 14627, USA
[51] The Rockefeller University, New York, New York 10021, USA
[52] Istituto Nazionale di Fisica Nucleare, Sezione di Roma 1,
[ii] Sapienza Università di Roma, I-00185 Roma, Italy
[53] Rutgers University, Piscataway, New Jersey 08855, USA
[54] Texas A&M University, College Station, Texas 77843, USA
[55] Istituto Nazionale di Fisica Nucleare Trieste/Udine,
I-34100 Trieste, [jj] University of Trieste/Udine, I-33100 Udine, Italy
[56] University of Tsukuba, Tsukuba, Ibaraki 305, Japan
[57] Tufts University, Medford, Massachusetts 02155, USA
[58] Waseda University, Tokyo 169, Japan
[59] Wayne State University, Detroit, Michigan 48201, USA
[60] University of Wisconsin, Madison, Wisconsin 53706, USA
[61] Yale University, New Haven, Connecticut 06520, USA

Using data from 2.9 fb^{-1} of integrated luminosity collected with the CDF II detector at the Tevatron, we search for resonances decaying into a pair of on-shell gauge bosons, WW or WZ, where one W decays into an electron and a neutrino, and the other boson decays into two jets. We observed no statistically significant excess above the expected standard model background, and we set cross section limits at 95% confidence level on G^* (Randall-Sundrum graviton), Z', and W' bosons. By comparing these limits to theoretical cross sections, mass exclusion regions for the three particles are derived. The mass exclusion regions for Z' and W' are further evaluated as a function of their gauge coupling strength.

PACS numbers: 14.70.Pw, 13.85.Rm, 13.85.Qk, 14.80.-j

Some models of new physics beyond the standard model predict particles that decay into pairs of on-shell bosons, for example Z', W'[1], or the Randall-Sundrum graviton G^* [2]. Searches for these particles in different decay channels have been reported elsewhere [3–7]. Most of them used final states consisting of only leptons or photons. In this Letter we search for these particles in the form of diboson resonances where one boson is a W decaying into an electron and a neutrino, and the other is a W or Z which decays into two jets. This search has the advantage of detecting two types of diboson resonances, WW and WZ, with the same final-state topology. The hadronic decay mode of the W or Z to two jets has a higher branching fraction compared to the leptonic mode; however, the background from jets also increases. Thus we implement a selection based on transverse energy (E_T) [8] of the detected objects in the final state to reduce standard model backgrounds and enhance sensitivity.

The diboson decay modes of Z' and W' directly probe the gauge coupling strength between the new and the standard model gauge bosons. The coupling strength strongly influences the decay branching ratios and the natural widths of the new gauge bosons. In an extended gauge model theory [1] the standard model coupling strength, $g \cdot \cos\theta_w$, is replaced by $\xi \cdot g \cdot \cos\theta_w$, where $\xi = C \cdot (M_W/M_V)^2$; C is a parameter that sets the coupling strength; and M_V is the mass of the new gauge boson, Z' or W'. We set cross section limits on Z' and W' as a function of mass and of ξ. Our results extend the sensitivity beyond the CDF Run I W' results [9] with almost 30 times the integrated luminosity, and, for the first time, set Z' limits as a function of mass and gauge coupling strength. For G^*, the coupling constant $k/\overline{M}_{Pl}$ dictates the branching ratio and natural width [2], where k and $\overline{M}_{Pl}$ are respectively the curvature of the extra dimension and the reduced Planck mass scale. This is also the first search for the G^* in the WW decay mode.

This analysis is based on data corresponding to an integrated luminosity of 2.9 fb^{-1} collected using the CDF II detector between March 2002 and February 2008. The detector is approximately forward-backward and azimuthally symmetric. The detector elements relevant to this analysis are the tracking system and the calorimeters. The tracking system consists of an eight-layer silicon tracker [10] surrounded by a 96-layer open-cell drift chamber (COT) [11]. The fiducial coverage of the COT is $|\eta| < 1.0$ [8], and the silicon detector extends the coverage to $|\eta| < 2.0$. The integrated tracking system is contained within a superconducting solenoid, providing a 1.4 T magnetic field. Surrounding the tracking system are the electromagnetic (EM) and hadronic calorimeters [12], divided into "central" ($|\eta| < 1.1$) and "plug" ($1.1 < |\eta| < 3.6$) regions. The calorimeters are made of lead (EM) and iron (hadronic) absorbers sandwiched between plastic scintillators that provide measurements of shower energies. At approximately the shower maximum, the EM calorimeters contain fine-grained detectors [13] for measuring shower positions and profiles.

As we are looking for events with an electron, a neutrino, and two jets, we start with data that were collected with an online selection requirement of a central electron with $|\eta| < 1$ and $E_T > 18$ GeV. From this dataset we select events that have an isolated electron [14] with $E_T > 30$ GeV, a neutrino identified by the requirement that the missing $E_T(\not\!\!E_T) > 30$ GeV, two or three jets with $|\eta| < 2.5$ and $E_T > 30$ GeV, and an overall $H_T > 150$ GeV, where H_T is the scalar sum of the electron E_T, the $\not\!\!E_T$, and the E_T of all jets [15].

To form a WW or WZ hypothesis for the selected events, the electron and $\not\!\!E_T$ are first combined to form a W candidate. Because the longitudinal component of the neutrino momentum (E_z^ν) is not available, the invariant mass of the electron and $\not\!\!E_T$ is artificially set to the W mass. With this assumption, the conservation of energy and momentum results in a quadratic equation for E_z^ν. If the discriminant of the quadratic equation is negative, the combination is discarded. If it is positive, there are two solutions and both are kept. In addition, two jets are combined to form a second W candidate or a Z candidate. In the case of a W candidate, we require the two-jet invariant mass (M_{jj}) to fall between 65 and 95 GeV/c^2, corresponding to $\pm 1.5\sigma$ of the expected reconstructed W

*Deceased
†With visitors from [a]University of Massachusetts Amherst, Amherst, Massachusetts 01003, [b]Universiteit Antwerpen, B-2610 Antwerp, Belgium, [c]University of Bristol, Bristol BS8 1TL, United Kingdom, [d]Chinese Academy of Sciences, Beijing 100864, China, [e]Istituto Nazionale di Fisica Nucleare, Sezione di Cagliari, 09042 Monserrato (Cagliari), Italy, [f]University of California Irvine, Irvine, CA 92697, [g]University of California Santa Cruz, Santa Cruz, CA 95064, [h]Cornell University, Ithaca, NY 14853, [i]University of Cyprus, Nicosia CY-1678, Cyprus, [j]University College Dublin, Dublin 4, Ireland, [k]University of Edinburgh, Edinburgh EH9 3JZ, United Kingdom, [l]University of Fukui, Fukui City, Fukui Prefecture, Japan 910-0017, [m]Kinki University, Higashi-Osaka City, Japan 577-8502, [n]Universidad Iberoamericana, Mexico D.F., Mexico, [o]University of Iowa, Iowa City, IA 52242, [p]Kansas State University, Manhattan, KS 66506, [q]Queen Mary, University of London, London, E1 4NS, England, [r]University of Manchester, Manchester M13 9PL, England, [s]Muons, Inc., Batavia, IL 60510, [t]Nagasaki Institute of Applied Science, Nagasaki, Japan, [u]University of Notre Dame, Notre Dame, IN 46556, [v]Obninsk State University, Obninsk, Russia, [w]University de Oviedo, E-33007 Oviedo, Spain, [x]Texas Tech University, Lubbock, TX 79609, [y]IFIC(CSIC-Universitat de Valencia), 56071 Valencia, Spain, [z]Universidad Tecnica Federico Santa Maria, 110v Valparaiso, Chile, [aa]University of Virginia, Charlottesville, VA 22906, [bb]Bergische Universität Wuppertal, 42097 Wuppertal, Germany, [cc]Yarmouk University, Irbid 211-63, Jordan, [kk]On leave from J. Stefan Institute, Ljubljana, Slovenia,

resolution. In the case of a Z candidate, this window is between 75 and 105 GeV/c^2. For a three-jet event, there are three two-jet invariant mass combinations. In this case only the pair with the invariant mass closest to either the W or the Z mass is kept in order to reduce the combinatorial background. The reconstructed W or Z candidates are then combined to form the final WW or WZ invariant mass.

Twelve standard model processes are considered as background for this analysis: $W(\rightarrow e^{\pm}\nu)$+jets, QCD jets, $t\bar{t}$, WW, $Z(\rightarrow e^+e^-)$+jets, $W(\rightarrow \tau^{\pm}\nu)$+jets, single top, WZ, $W\gamma$, $Z \rightarrow \tau^+\tau^-$, $\gamma\gamma$, and ZZ. The dominating background is W+jets whose contribution is estimated by Monte Carlo simulation using the ALPGEN [16] event generator, interfaced to PYTHIA [17] for parton showering and followed by the GEANT 3 [18] based CDF II detector simulation. With the exception of the QCD jet background, the rest of the background processes are all estimated by Monte Carlo simulation using the PYTHIA event generator. The cross sections used for the simulated background processes are obtained from NLO calculations.

The QCD jet background comes from events with three or more jets where one of the jets is misidentified as an electron. With this misidentified electron, the event may pass through subsequent event selection criteria and the reconstruction processes. The contribution of the QCD jet background is estimated using a dataset that has an online selection requirement of one jet with $E_T > 20$ GeV. We first exclude events that have any identified electrons, then each jet in the central region is treated as an electron with a weight corresponding to the probability that a jet is misidentified as an electron. This probability is a function of jet E_T and varies from 10^{-4} at 30 GeV to 10^{-3} above 100 GeV [6]. The misidentified electron is combined with the $\not\!\!E_T$ and then with two jets to form WW or WZ candidates as described earlier. The resulting QCD jet background is normalized to the data by matching the $\not\!\!E_T$ spectrum between data and expected background at their peaks around 10 GeV, where little signal is expected and the QCD jet background dominates. This normalization factor is used for the QCD jet contribution throughout the analysis. Figure 1 shows the resulting $\not\!\!E_T$ spectrum for events with two jets that would have passed the event selection criteria except for the $\not\!\!E_T > 30$ GeV cut.

The systematic uncertainties taken into account in the background calculations are the following, listed by decreasing significance: jet energy scale (JES) uncertainty [19], theoretical cross section uncertainty [20], luminosity uncertainty [21], and jet misidentification rate uncertainty. The dominating systematic uncertainty is the JES uncertainty which amounts to $\sim 13\%$ of the estimated background. The cross section and luminosity uncertainties are $\sim 6\%$ each.

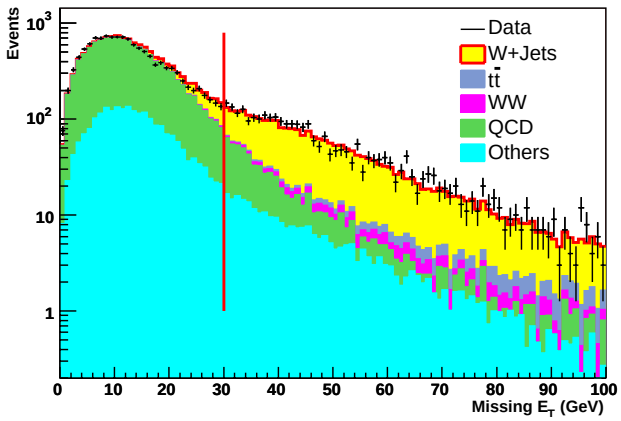

FIG. 1: $\not\!\!E_T$ spectrum from events with two jets. The vertical line marks the $\not\!\!E_T > 30$ GeV cut. The QCD component is scaled such that data and expected background match at the peak area where no signal is expected. "Others" background includes: $Z(\rightarrow e^+e^-)$+jets, single top, WZ, $W\gamma$, $Z \rightarrow \tau^+\tau^-$, $\gamma\gamma$, and ZZ.

Signal detection efficiencies are also determined from simulated events using the PYTHIA event generator. For a set of selected mass values ranging from 165 GeV/c^2 to 1000 GeV/c^2, the three types of particles are simulated: G^* with $k/\overline{M}_{Pl} = 0.1$, Z' and W' with PYTHIA default settings corresponding to the extended gauge model with a suppression factor $\xi = (M_W/M_V)^2$, i.e., $C = 1$. The reconstructed signals are Gaussian in shape, and the mass resolution is linearly proportional to the generated mass values, varying from 20 GeV/c^2 at 200 GeV/c^2 mass to 80 GeV/c^2 at 1000 GeV/c^2 mass. For calculating the efficiencies we choose an acceptance mass window corresponding to ± 1.5 times the reconstructed signal resolution. This choice gives a good signal to background ratio. The same acceptance mass windows are also used to obtain the number of background events.

The systematic uncertainties taken into account for the signal acceptance, defined as the product of signal detection efficiency and integrated luminosity, in order of decreasing significance, are: jet energy scale (JES) uncertainty, luminosity uncertainty, initial state radiation (ISR) uncertainty, final state radiation (FSR) uncertainty, and parton distribution function (PDF) uncertainty. Similarly to the background uncertainties, the JES uncertainty dominates the systematic uncertainties and varies from 12% at 170 GeV/c^2 mass to 6% at 700 GeV/c^2 mass for G^*, 13% (170 GeV/c^2) to 6% (1000 GeV/c^2) for Z', and 9% (190 GeV/c^2) to 6% (1000 GeV/c^2) for W'. ISR, FSR and PDF uncertainties are of the order of $1-3\%$ each and decrease with increasing diboson mass.

In order to improve sensitivity at higher mass, addi-

tional sets of higher E_T cuts for the constituent particles (observed in the detector as electron, $\not\!\!E_T$ from neutrino, and jets) are tried. Two series of the E_T cut sets are implemented. The first series requires a higher E_T on all four participating particles ranging from 40 GeV to 80 GeV in steps of 10 GeV. The second series requires a higher E_T on only one daughter particle from each of the decaying bosons, i.e., a higher E_T for either the electron or the neutrino, and the same higher E_T for one of the two jets. The E_T values in this series range from 40 GeV to 120 GeV in steps of 10 GeV. For each set of E_T cuts the systematic uncertainties for the backgrounds and the acceptances are re-evaluated, but are found to be not very sensitive to the variations.

To find the optimal set of E_T cuts at each selected mass point, the expected cross section limits, which are based only on the background and the signal acceptance, are calculated for each set of cuts. We found that the first series of E_T cuts gives the best expected limits for Z' and W', while the second series is best for G^*. The optimal E_T cuts for each particle type are then selected from their own optimal series. The sets that give the best expected limits are chosen without reference to their impact on the data sample. Although the background processes respond differently to the two series of E_T cuts, the best expected limits obtained from each series are very similar. Generally, as the mass increases the higher E_T cuts yield better expected limits.

We use a Bayesian method [22] to calculate cross section limits. Inputs to the calculation are signal acceptance, estimated background, and observed data. The signal acceptance and background are assigned priors and modeled via a Monte Carlo method that allows correlation of uncertainties between acceptance and background. In our analysis, the JES and luminosity uncertainties in the acceptance and in the background are correlated. The expected limits are calculated by simulating observed data based on the expected background with Poisson fluctuations.

Figure 2 shows typical invariant mass distributions reconstructed for each particle type for a mass of 600 GeV/c^2 using the optimal set of E_T cuts in each case. The WW invariant mass distributions are shown for G^* and Z', and the WZ invariant mass distribution is shown for W'. The optimal set of E_T cuts for G^* at 600 GeV/c^2 is from the second series with $E_T > 120$ GeV, while both Z' and W' favor the first series with $E_T > 60$ GeV. The background compositions, as shown in Table I, are found to be more sensitive to the different sets of E_T cuts than to the different decay types (WW or WZ). For Z' and W', the QCD jet background has a much lower contribution owing to the stricter E_T requirements.

Without a statistically significant excess above the expected background in the invariant mass plots, we calculate the cross section limits at 95% confidence level (C.L.) for the observed data. Figure 3 shows the observed and the expected 95% C.L. cross section limits overlaid with theoretical cross sections. The theoretical cross sections for G^* and Z' are calculated from PYTHIA version 6.216, and a constant K-factor of 1.3 is applied to take into account the NLO correction [4–6]. The theoretical cross section for W' is derived from a NLO calculation [23]. The upper right inserts in Fig. 3 show ratios of the limits to the theoretical cross sections. Where the ratio is below one the mass region is excluded. Table II summarizes the mass exclusion regions from the figures.

TABLE I: Percentage fractional background compositions in Fig. 2. The uncertainties include both statistical and systematic uncertainties.

	$G^*(WW)$	$Z'(WW)$	$W'(WZ)$
W+jets	31.8 ± 8.2	33.0 ± 10.0	36.8 ± 9.7
$t\bar{t}$	19.6 ± 2.7	35.1 ± 4.0	37.4 ± 5.2
WW	10.7 ± 3.2	15.2 ± 2.8	13.4 ± 3.2
QCD jets	32.7 ± 6.5	5.1 ± 1.0	5.6 ± 1.1
Others	5.3 ± 0.9	2.4 ± 0.9	3.4 ± 1.0

TABLE II: Mass exclusion region at 95% C.L. with $k/\overline{M}_{Pl} = 0.1$ for G^*, and $\xi = (M_W/M_V)^2$ ($C = 1$) for Z' and W'.

	G^*	Z'	W'
Expected Exclusion (GeV/c^2)	< 632	257-630	381-421
Observed Exclusion (GeV/c^2)	< 607	247-544	285-516

The results shown in Fig. 3 and Table II for Z' and W' are based on a gauge coupling mixing factor of $\xi = C \cdot (M_W/M_V)^2$, with $C = 1$. Since signal acceptance is the only quantity that changes with ξ in the cross section limit calculation, at each mass point we re-evaluate signal acceptances for different ξ values and calculate cross section limits as a function of ξ. Comparing the calculated and theoretical cross sections as a function of ξ, a ξ exclusion region is derived at each mass point. These Z' and W' exclusion regions are shown in Fig. 4. The branching ratio of Z' or W' to fermions decreases as ξ increases. This is opposite to the diboson decay modes where branching ratios increase as ξ increases. Most Z' or W' search results [6, 7] report mass limits along the $\xi = (M_W/M_V)^2$ line and we have also done so for comparison. However, the diboson decay modes and the fermionic decay modes are sensitive to different parts of the gauge coupling strength phase space, so searches for bosonic and fermionic decays of Z' and W' are complementary to each other. The W' result shown in Fig. 4 is significantly improved compared to the previous result from CDF Run I [9]. The Z' result shown is the first to

set an exclusion region as a function of ξ and mass.

In conclusion, we have searched for new particles decaying into a pair of bosons in the electron, $\not\!\!E_T$, and two jets final state. In data from an integrated luminosity of 2.9 fb^{-1}, no significant excess over the standard model prediction is observed. Cross section limits at 95% C.L. and mass exclusion regions have been obtained for a Randall-Sundrum graviton, Z' and W' bosons. The W' exclusion region in the $\xi - M_{W'}$ plane has been extended significantly compared to the previous measurement. We have also presented the Z' exclusion region in the $\xi - M_{Z'}$ plane for the first time. We set the most stringent mass limits on W' and Z' bosons.

We thank the Fermilab staff and the technical staffs of the participating institutions for their vital contributions. This work was supported by the U.S. Department of Energy and National Science Foundation; the Italian Istituto Nazionale di Fisica Nucleare; the Ministry of Education, Culture, Sports, Science and Technology of Japan; the Natural Sciences and Engineering Research Council of Canada; the National Science Council of the Republic of China; the Swiss National Science Foundation; the A.P. Sloan Foundation; the Bundesministerium für Bildung und Forschung, Germany; the World Class University Program, the National Research Foundation of Korea; the Science and Technology Facilities Council and the Royal Society, UK; the Institut National de Physique Nucleaire et Physique des Particules/CNRS; the Russian Foundation for Basic Research; the Ministerio de Ciencia e Innovación, and Programa Consolider-Ingenio 2010, Spain; the Slovak R&D Agency; and the Academy of Finland.

[1] G. Altarelli, B. Mele, and M. Ruiz-Altaba, Z. Phys. **C45**, 109 (1989).

[2] L. Randall and R. Sundrum, Phys. Rev. Lett. **83**, 3370 (1999).

[3] J. Alcaraz *et al.* [ALEPH, DELPHI, L3, OPAL Collaborations, LEP Electroweak Working Group], arXiv:hep-ex/0612034v2, "A Combination of Prelimixnary Electroweak Measurements and Constraints on the Standard Model."

[4] T. Aaltonen *et al.* (CDF collaboration), Phys. Rev. Lett. **99**, 171801 (2007).

[5] T. Aaltonen *et al.* (CDF collaboration), Phys. Rev. Lett. **99**, 171802 (2007).

[6] T. Aaltonen *et al.* (CDF collaboration), Phys. Rev. Lett. **102**, 031801 (2009).

[7] V.M. Abazov *et al.* (D0 collaboration), Phys. Rev. Lett. **100**, 031804 (2008).

[8] D. Acosta *et al.*, Phys. Rev. D **71**, 032001 (2005). CDF uses a cylindrical coordinate system in which $+z$ points along the direction of the proton beam, r is the radius from the nominal beam line, and ϕ is the azimuthal angle. The pseudorapidity is defined as $\eta = -\ln[\tan(\theta/2)]$, where θ is the polar angle measured from the $+z$ axis. Transverse energy is defined as $E_T = E \cdot \sin\theta$, where E is the measured calorimeter energy. Transverse momentum is defined as $p_T = p \cdot \sin\theta$, with p being the track momentum.

[9] T. Affolder *et al.* (CDF collaboration), Phys. Rev. Lett. **88**, 071806 (2002).

[10] A. Sill *et al.*, Nucl. Instrum. Methods Phys. Res. Sect. A **447**, 1 (2000).

[11] T. Affolder *et al.*, Nucl. Instrum. Methods Phys. Res. Sect. A **526**, 249 (2004).

[12] L. Balka *et al.*, Nucl. Instrum. Methods Phys. Res. Sect. A **267**, 272 (1988); S. Bertolucci *et al.*, Nucl. Instrum. Methods Phys. Res. Sect. A **267**, 301 (1988); M. Albrow *et al.*, Nucl. Instrum. Methods Phys. Res. Sect. A **480**, 524 (2002).

[13] G. Apollinari *et al.*, Nucl. Instrum. Methods Phys. Res. Sect. A **412**, 515 (1998).

[14] Electrons are isolated if in a surrounding cone of 0.4 radius the E_T deposited is no more than 1.1 times the electron E_T in the EM calorimeters.

[15] F. Abe *et al.* (CDF collaboration), Phys. Rev. Lett. **75**, 3997 (1995).

[16] M.L. Mangano, M. Moretti, F. Piccinini, R. Pittau, and A. Polosa, J. High Energy Phys. **0307** (2003) 001.

[17] T. Sjostrand *et al.*, Comput. Phys. Commun. **135**, 238 (2001).

[18] S. Agostinelli *et al.*, Nucl. Instrum. Methods Phys. Res. Sect. A **506**, 250 (2003).

[19] A. Bhatti *et al.*, Nucl. Instrum. Methods Phys. Res. Sect. A **566**, 375 (2006).

[20] U. Baur, T. Han, and J. Ohnemus, Phys. Rev. D **48**, 5140 (1993); J. M. Campbell and R. K. Ellis, Phys. Rev. D **60**, 113006 (1999).

[21] D. Acosta *et al.*, Nucl. Instrum. Methods Phys. Res. Sect. A **494**, 57 (2002).

[22] J. Heinrich *et al.*, arXiv:physics/0409129, "Interval estimation in the presence of nuisance parameters. 1. Baysian approach."

[23] Z. Sullivan, Phys. Rev. D **66**, 075011 (2002).

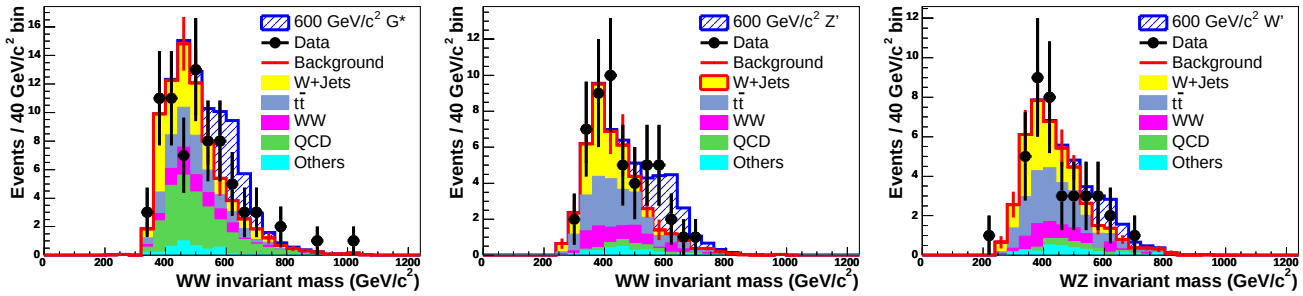

FIG. 2: Invariant mass distributions with optimal set of E_T cuts for 600 GeV/c^2 signals. Left to right: $G^*(WW)$, $Z'(WW)$, $W'(WZ)$. G^* and Z' are the same decay mode (WW) but with different optimal selections. Z' and W' have the same optimal selection but different decay modes (WW vs WZ). Superimposed on top of the backgrounds are signals at 600 GeV/c^2 mass corresponding to the theoretical cross sections.

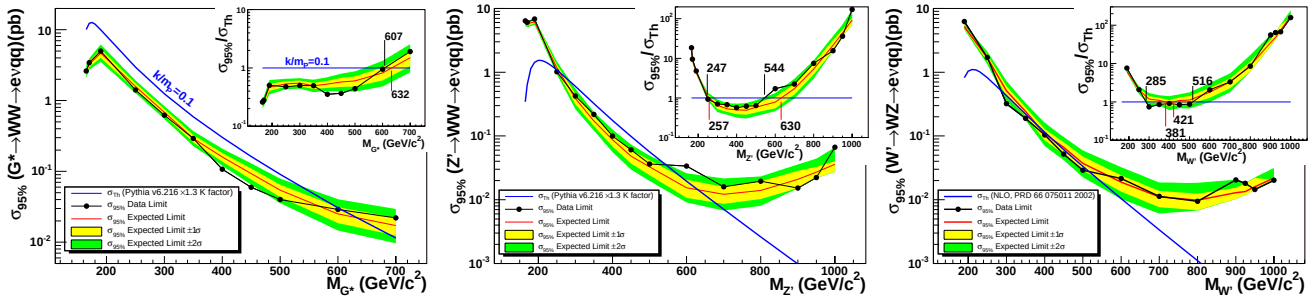

FIG. 3: Cross section limits at 95% C.L. Left to right: G^*, Z', W'. Inserts at upper right are cross section limits divided by the theoretical cross sections. Yellow and green bands show 1σ and 2σ bands on the expected limits, respectively.

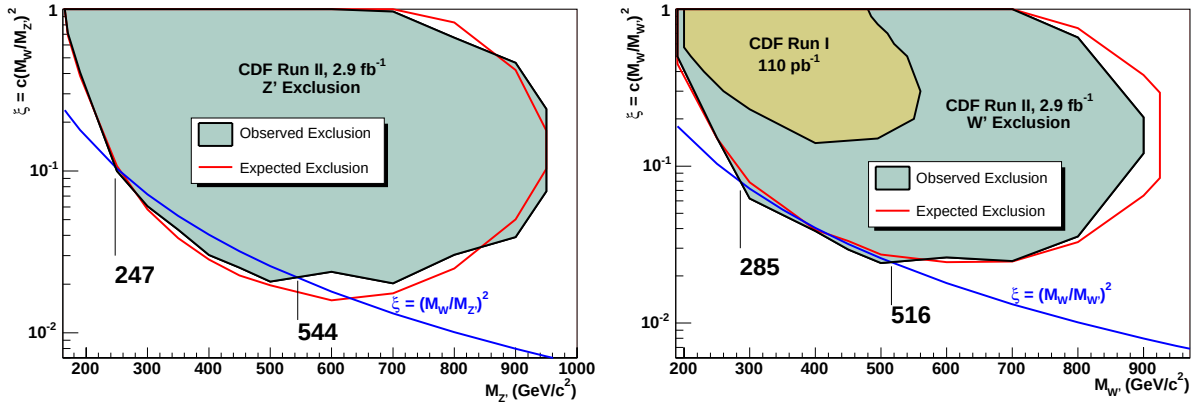

FIG. 4: Z' (left) and W' (right) exclusion regions as a function of mass and ξ. The $\xi = (M_W/M_V)^2$ (i.e., $C = 1$) lines indicate PYTHIA defaults and are commonly used for mass exclusion regions. The vertical lines mark the results as shown in Table II. Also shown in the W' plot is the CDF Run I result.